POLARIZATION ENHANCED NQR DETECTION AT LOW FREQUENCIES

Janko Lužnik, Janez Pirnat, Vojko Jazbinšek and Zvonko Trontelj
Institute of Mathematics, Physics and Mechanics, Ljubljana, Slovenia

Tomaž Apih, Alan Gregorovič and Robert Blinc
J. Stefan Institute, Ljubljana, Slovenia

Janez Seliger
Faculty of Mathematics and Physics, University of Ljubljana, Slovenia

Abstract

In this contribution we present our current research on polarization enhanced nuclear quadrupole resonance (NQR) detection at low frequencies with the emphasis on ^{14}N NQR trinitrotoluene (TNT) detection at room temperature. Combination of proton-nitrogen level crossing polarization transfer and pulsed spin-locking sequence makes ^{14}N NQR in TNT fast and sensitive enough to be used in routine detection of explosives. Enhancement factors for ^{14}N NQR lines in TNT were calculated and compared with experimental values. Good agreement between measured and calculated signal enhancement factors was observed. ^{14}N NQR signals in a 15 g trinitrotoluene sample of predominantly monoclinic modification were measured in 15 s in different polarization magnetic fields. The conditions for optimal polarization enhancement were determined.

Introduction

Nuclear Quadrupole Resonance (NQR), with its ability to identify specific molecules, is potentially a powerful method in solid state physics, chemistry and pharmacy. In the last 10 to 15 years, several attempts have been made to improve the detection of military explosives, improvised explosive devices (IED) and other illicit materials – mainly narcotics - by ^{14}N NQR [1-9]. Unfortunately, many of these substances have ^{14}N NQR frequencies in the low frequency domain between 100 and 1000 kHz, hence a rather low signal to noise (s/n) ratio. Therefore, the measuring times for the required signal averaging can be hours and they are thus too long for practical applications. With a combination of proton polarization transfer to nitrogen nuclei and multi-pulse spin-locking sequences the measuring time can be significantly reduced to an acceptable level of the order of 10 s, provided the proton and the nitrogen spin-lattice relaxation times (T_1) are suitable.

There are two ways to increase the s/n ratio by proton-nitrogen level crossing polarization transfer: a) proton-nitrogen nuclear double resonance techniques [10-13] using changes in the proton NMR signal as an indirect indication of the ^{14}N NQR transitions; and b) direct ^{14}N NQR detection where the signal is enhanced by proton polarization transfer via proton-nitrogen level crossing in a time variable magnetic field [14-19]. The first technique requires a homogeneous applied external magnetic field and is therefore not convenient for work in the

field. For direct ^{14}N NQR detection there is no requirement for homogeneity of the polarizing magnetic field, because the signal enhancement depends on the average magnetic field, while pure NQR detection is performed in a zero magnetic field.

The aim of this study was to find a combination of polarization enhanced (PE) ^{14}N NQR detection together with a suitable pulse sequence in pulsed NQR spectroscopy to obtain low frequency ^{14}N NQR signals in TNT at room temperature in 10 to 20 s.

Theoretical

In NQR (NMR) spectroscopy signal intensities are limited by the difference in the occupation number ΔN between two energy levels [20-22]. In thermal equilibrium the occupation of different energy levels follows the Boltzmann distribution function

$$N \propto \exp\left(-\frac{E}{k_B T}\right) \tag{1}$$

Knowing that in rf spectroscopy the high temperature limit ($k_B T >> E$) is applicable, the population difference between two energy levels is:

$$\Delta N_Q \propto \frac{\Delta E}{k_B T} = \frac{h\nu_Q}{k_B T} \tag{2}$$

The population difference is thus proportional to the NQR transition frequency:

$$\Delta N_Q \propto \nu_Q$$

This population difference can be increased by applying cross polarization transfer. When the measured sample contains also protons, their spins can be polarised in a strong magnetic field. Consequently the population difference for protons is:

$$\Delta N_H \propto \gamma B \propto h\nu_H \; ; \qquad \Delta N_H \propto \nu_H \tag{3}$$

For strong polarizing magnetic fields where $\nu_H >> \nu_Q$ also $\Delta N_H >> \Delta N_Q$ (ν_H is the proton NMR transition frequency in the polarizing magnetic field B). After proton polarization is complete – the polarization time should be longer than T_1 of the protons – the polarizing magnetic field is adiabatically removed. This field can be obtained either with an electromagnet or with a suitable permanent magnet. During demagnetization the proton NMR transition frequency goes to zero, but the energy levels population difference for protons remain temporarily unbalanced and available for improvement of the ^{14}N NQR signal in a time short compared to the proton spin-lattice relaxation time T_1. In the adiabatic demagnetization process the proton NMR and the nitrogen NQR transition frequencies become equal (level crossing), and the relative population differences ΔN_H for protons and ΔN_Q for nitrogens equalize due to the proton-

nitrogen dipolar coupling. The population differences ΔN_H and ΔN_Q are proportionally distributed between protons and nitrogens. A new average population difference can be defined as:

$$\Delta N = \frac{N_H \Delta N_H + N_N \Delta N_Q}{N_H + N_N} = (1-\rho)\Delta N_H + \rho \Delta N_Q \tag{4}$$

Where N_H and N_N are the numbers of protons and nitrogen nuclei in the molecule of the sample and

$$\rho = \frac{N_N}{N_H + N_N} \tag{5}$$

Using a pulse NQR spectrometer in a zero magnetic field and triggering it immediately after demagnetization is completed, under optimal conditions this enhancement factor for the quadrupole signal intensity can be obtained

$$EF = \frac{\Delta N}{\Delta N_Q} = (1-\rho)\frac{\Delta N_H}{\Delta N_Q} + \rho = (1-\rho)\frac{\nu_H}{\nu_Q} + \rho \tag{6}$$

The case spin I=1 ^{14}N nuclei with $\eta \neq 0$: The allowed transitions and energy levels for this case are shown in Fig. 1. The corresponding frequencies are equal to [22]:

$$\nu^+ = \frac{3e^2qQ}{4h}\left(1+\frac{\eta}{3}\right), \quad \nu^- = \frac{3e^2qQ}{4h}\left(1-\frac{\eta}{3}\right) \quad \text{and} \quad \nu^0 = \frac{e^2qQ}{2h}\eta \tag{7}$$

Here, e^2qQ/h is the quadrupole coupling constant where Q is the nuclear electric quadrupole moment, $q = q_{zz}$ is the maximal component of the electric field gradient tensor, e is the electron charge, h the Planck constant, and $\eta = (q_{xx} - q_{yy})/q$ is the asymmetry parameter.

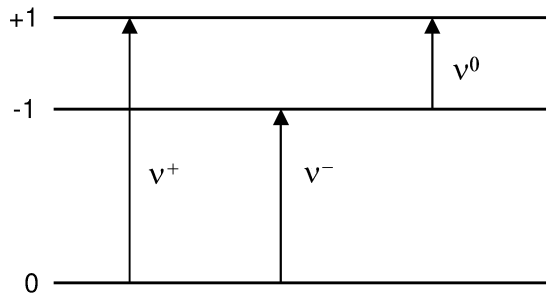

Figure 1: The quadrupole energy levels and allowed transitions for a spin 1 nucleus

In the case I = 1 the polarization transfer is a three step process [18] with successive crossings of energy levels: ν^+ (step I), ν^- (step II) and ν^0 (step III) as

illustrated in Fig. 2. During this process, the "step-by-step" alterations of relative population numbers are given as the differences from the uniform distribution (1/3 of the nuclei in each energy level). Throughout the following is valid:

$$N_i^0 + N_i^- + N_i^+ = N \Rightarrow \Delta N_i^0 + \Delta N_i^- + \Delta N_i^+ = 0 \tag{8}$$

The initial condition is:

$$\Delta N_0^0 - \Delta N_0^+ = Nh\nu^+ / 3k_BT = k\nu^+ \qquad \Delta N_0^0 - \Delta N_0^- = Nh\nu^- / 3k_BT = k\nu^- \tag{9}$$

N is the total number of nitrogen nuclei and $k = Nh / 3k_BT$.

In the calculation also alterations in the proton reservoir after each level crossing are considered. The following results for α, β and γ, introduced in Fig.2 and describing the gradual population changes are obtained:

$$\begin{aligned}
\alpha &= (\nu_H - \nu^+)(1-\rho) \\
\beta &= \frac{1}{2}(\nu_H - \nu^+)(1-\rho)^2 + (1-\rho)\nu^0 \\
\gamma &= \frac{3}{4}(\nu_H - \nu^+)(1-\rho)^3 + (1-\rho)(\nu^- - \nu^0) + \frac{3}{2}(1-\rho)^2\nu^0
\end{aligned} \tag{10}$$

The enhancement factors for ν^+, ν^- and ν^0 of ^{14}N NQR signal intensities are the ratios of the final and initial population differences:

$$EF^+ = \Delta N_3^+ / \Delta N_0^+ = (\nu^+ + \alpha + \beta/2 + \gamma/2) / \nu^+$$

$$EF^- = \Delta N_3^- / \Delta N_0^- = (\nu^- + \alpha/2 + \beta - \gamma/2) / \nu^-$$

$$EF^0 = \Delta N_3^0 / \Delta N_0^0 = (\nu^0 + \alpha/2 - \beta/2 + \gamma) / \nu^0$$

$$\begin{aligned}
EF^+ &= \frac{1+9\rho-5\rho^2+3\rho^3}{8} + \frac{13-21\rho+11\rho^2-3\rho^3}{8\nu^+}\nu_H + \frac{-2+8\rho-6\rho^2}{8\nu^+}\nu^- \\
EF^- &= \frac{-2+4\rho+6\rho^2}{8} + \frac{5-3\rho-5\rho^2+3\rho^3}{8\nu^-}\nu_H + \frac{1+3\rho-\rho^2-3\rho^3}{8\nu^-}\nu^+ \\
EF^0 &= \frac{-4\rho+12\rho^2}{8} + \frac{8-18\rho+16\rho^2-6\rho^3}{8\nu^0}\nu_H + \frac{10\rho-16\rho^2}{8\nu^0}\nu^+
\end{aligned} \tag{11}$$

In the calculation of enhancement factors an ideal adiabatic demagnetization and 100 % cross-polarization transfer effectiveness were assumed. In each level crossing only two of the three levels are involved, hence the effective number of nitrogen nuclei is only 2/3 of the total number and the value for ρ is:

$$\rho = \frac{\frac{2}{3}N_N}{N_H + \frac{2}{3}N_N} \qquad (12)$$

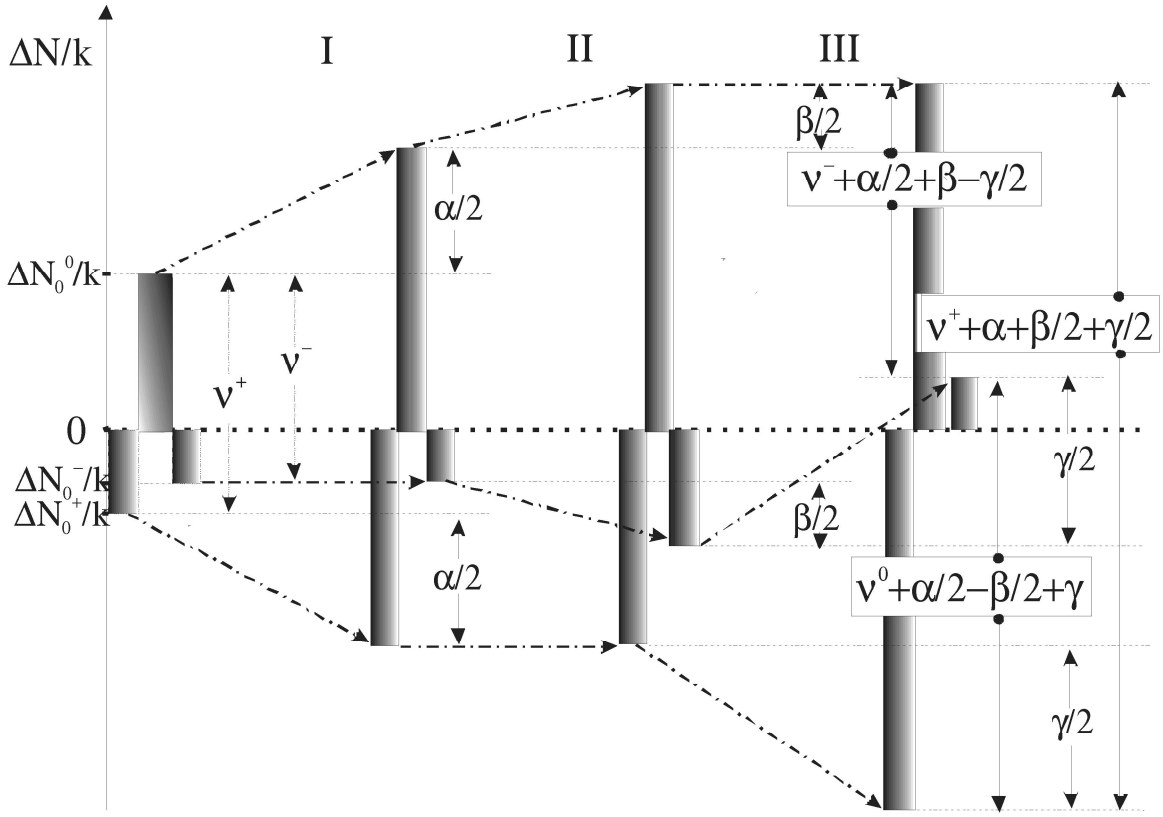

Figure 2: The occupation number alteration of different energy levels in a three step cross-polarization transfer. α, β and γ denote the increments of the population differences after each level crossing.

Experimental

In our experiments, protons in polycrystalline trinitrotoluene (TNT) sample were polarized by a block shaped NdFeB permanent magnet (70 mm x 65 mm x 65 mm). The polarizing device consisted of a computer controlled linear robotic arm, carrying the magnet towards and away from the sample. A cylindrical sample with diameter of 18 mm was at stable room temperature in modestly rf shielded space. In the nearest position the magnet was distant 10-12 mm from the sample surface. The vertical sample direction was perpendicular to the polarizing magnetic field. With this setup, it was possible to optimize the duration of level crossing. When the magnet is in the far position, its field value did not exceed the double value of the earth's magnetic field. The experimental procedure is shown schematically in Fig. 3. At time t = 0, protons were polarized in a strong magnetic field. Then the magnet was quickly moved away (adiabatic demagnetization - fast compared to the proton T_1). During the demagnetization procedure when the proton NMR frequency became equal successively to each of the three ^{14}N NQR frequencies, the polarization was transferred from protons

to nitrogen nuclei. Finally, in a zero magnetic field, standard pulsed spin-locking NQR detection was performed.

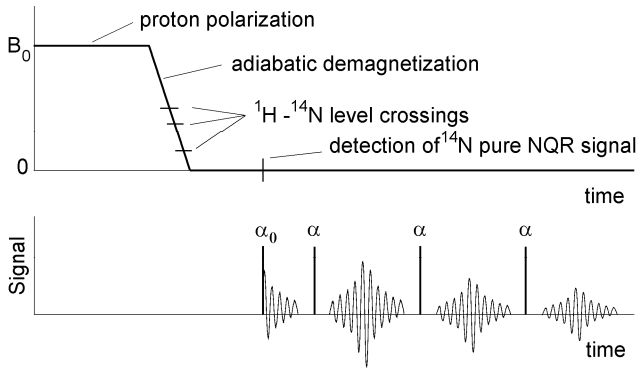

Figure 3: Proton-nitrogen level crossing polarization enhancement and pulsed spin-locking detection procedure (schematic).

Polarization enhanced NQR was tested by measuring the ^{14}N NQR spectrum of TNT ($C_7H_5O_6N_3$). TNT exists in two crystal modifications, orthorhombic and monoclinic, with six non-equivalent nitrogen sites giving six different sets of ν^+, ν^- and ν^0 ^{14}N NQR lines (Fig. 4) for each crystal modification. The monoclinic phase is considered to be the stable phase at room temperature [24-25]. TNT samples of different age and origin (Italian, German, Swiss, Czech and Yugoslav) were investigated. No significant differences were observed between them (Table 1). All samples were predominantly in the monoclinic phase, probably due to the remelting procedure which was generally carried out.

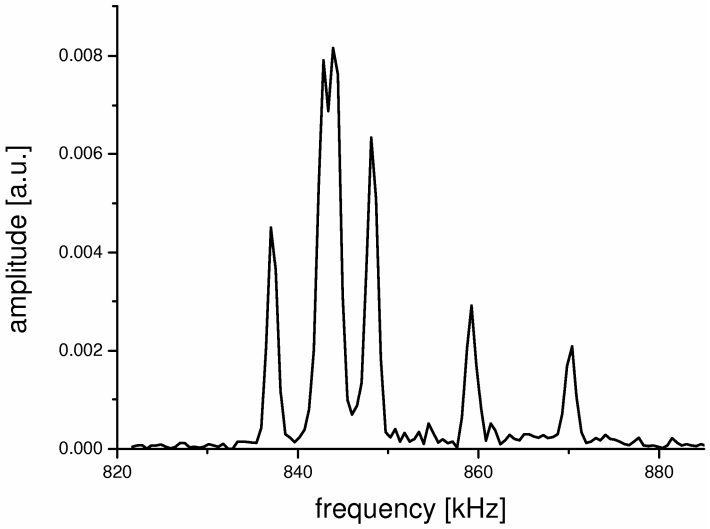

Figure 4: ν^+ part of ^{14}N NQR spectrum of predominantly monoclinic TNT. Six lines for monoclinic TNT can be resolved: 837 kHz, 842 kHz, 844 kHz, 848 kHz, 859 kHz and 870 kHz. This spectrum was obtained from nine averages in three sets where only the transmitter frequency was changed in three steps (837 kHz, 846 kHz and 865 kHz). The reference frequency Rx was constant at 855 kHz. A polarizing field of about 250±50 mT was used for this polarization enhancement experiment.

No.	ν^+[kHz]	ν^- [kHz]	ν^0 [kHz]	η
1	870	714	156	0.295
2	859	751	108	0.201
3	848	739	109	0.206
4	844	714	130	0.250
5	842	769	73	0.136
6	837	743	94	0.178

Table1: ^{14}N NQR frequencies and asymmetry parameters for monoclinic TNT at room temperature

Results and discussion

Having six different ν^+, ν^- and ν^0 ^{14}N NQR lines for this particular case means that each level crossing in the three-step polarization transfer is itself a six step process and exact calculation of the enhancement factor is much more complicated. However, if we taking into account the Zeeman broadening of ^{14}N NQR lines in polycrystalline or powder samples in the magnetic fields where the cross polarization transfer occurs, the transfer can be considered as a simultanous process for all six lines (12 lines for mixed samples), because the broadenings of the lines is much stronger than the distances between them [28]. Therefore, the three level model is very close to the real situation. For TNT we have $\rho = 2/7$ and the enhancement factors for ν^+, ν^- and ν^0 can be calculated (Fig. 5):

$$\begin{aligned} EF^+ &= 0.413 + 0.978\frac{\nu_H}{\nu^+} + 0.026\frac{\nu^-}{\nu^+} \\ EF^- &= -0.046 + 0.476\frac{\nu_H}{\nu^-} + 0.213\frac{\nu^+}{\nu^-} \\ EF^0 &= -0.020 + 0.503\frac{\nu_H}{\nu^0} + 0.211\frac{\nu^+}{\nu^0} \end{aligned} \qquad (13)$$

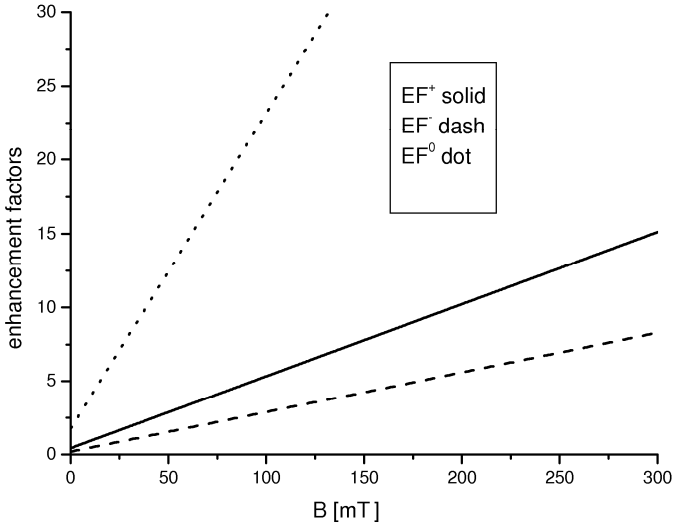

Figure 5: Calculated enhancement factor vs the polarizing field for ν^+, ν^- and ν^0 lines in TNT. Average enhancement factors for ν^+, ν^- and ν^0 are given assuming that ν^+ and ν^- transitions are grouped around 850 kHz and 750 kHz, respectively.

In polarization enhanced NQR detection the initial polarization time must be long enough to allow complete proton polarization, i.e. the proton polarization time T_{pol} must be long compared to the proton spin-lattice relaxation time T_1 ($T_{pol} >> T_1$). The proton T_1 in TNT strongly depends on temperature and the Zeeman magnetic field.[11] From an asymptotic approach to the maximal signal intensity of the ^{14}N NQR signal (Fig. 6) we estimated that T_1 of protons in a field of about 400 mT is about 16 s, which is in agreement with the reported measurements [17]. The required proton polarization time is thus around 30 s and this part of the measuring procedure is the most time consuming part of the whole experiment (Obviously, for lower polarization fields T_1 of protons is shorter and correspondingly also the required polarization time.).

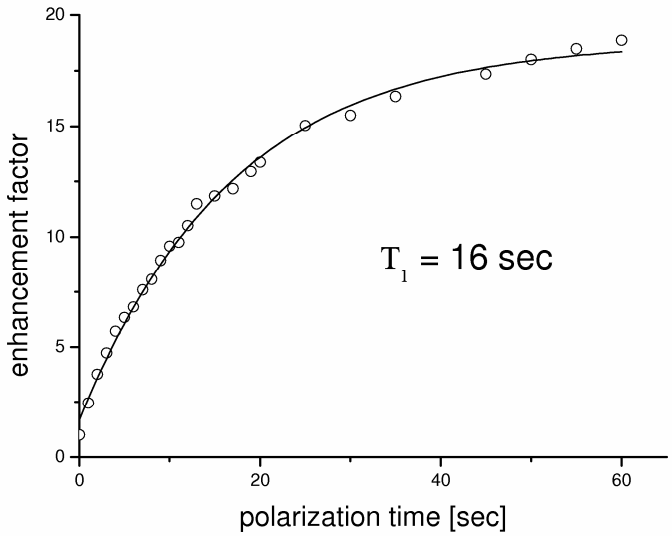

Figure 6: Average signal intensity vs polarization time for the triplet (842, 844 and 848 kHz) NQR line in the polarizing field 400±50 mT. The characteristic time for an exponential fit to the measured data is 16 s. This time is approximately equal to the proton spin-lattice relaxation time T_1.

Polarization of protons was followed by fast adiabatic demagnetization and the trigger onset for the beginning of the NQR pulse sequence was programmed at the point when zero magnetic field was reached. at the end of adiabatic demagnetization. The demagnetization times in our experiments (Fig. 7) were 300 ms to 500 ms and were short enough compared to the proton T_1. The time interval between the final level crossing and the trigger onset (at zero field) must be short compared to the nitrogen relaxation time T_{1N}. By altering the trigger delay we could estimate the nitrogen spin lattice relaxation times. For the ν^+ (average for triplet at 842, 844 and 848 kHz) transitions of the monoclinic TNT we obtained a T_{1N} of approximately 7 s at room temperature (Fig. 8).

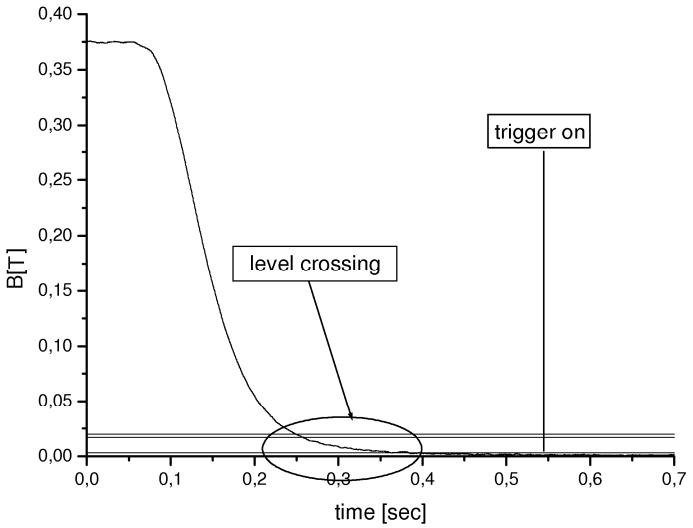

Figure 7: A typical time dependence of the magnetic field at the place of the sample.

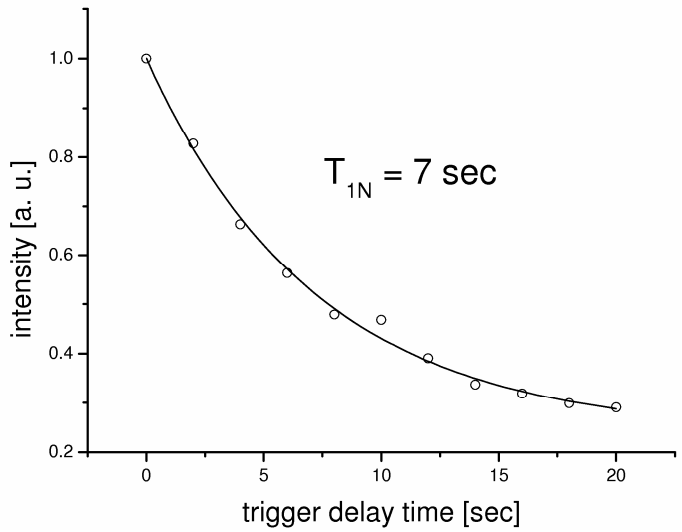

Figure 8: Average ^{14}N NQR signal intensity vs trigger delay time for the triplet line (842, 844 and 848 kHz) in TNT at room temperature.

The efficiency of cross-polarization transfer depends on the strength of the proton-nitrogen spin coupling ν_{NH}. For TNT ν_{NH} ~ 500 Hz [26]. For successful polarization transfer the cross-polarization time must be long compared to $1/\nu_{NH}$ ~ 2 ms, giving the limit for the field sweep speed dB/dt at level crossings. Considering that the proton NMR line-width $\Delta\nu_H$ is around 20 kHz (0.5 mT), we can write the condition:

$$dB/dt << 0{,}5 \text{ mT}/2 \text{ ms} = 250 \text{ mT/s}$$

In our experimental arrangement we were close to this limit (Fig. 9) and the experimental enhancement factors for PE NQR in TNT are close to the calculated ones in the ideal case. To confirm this we measured the signal intensity enhancement factor versus polarizing magnetic field (Fig. 10). The measured enhancement factor was only slightly lower than the calculated one.

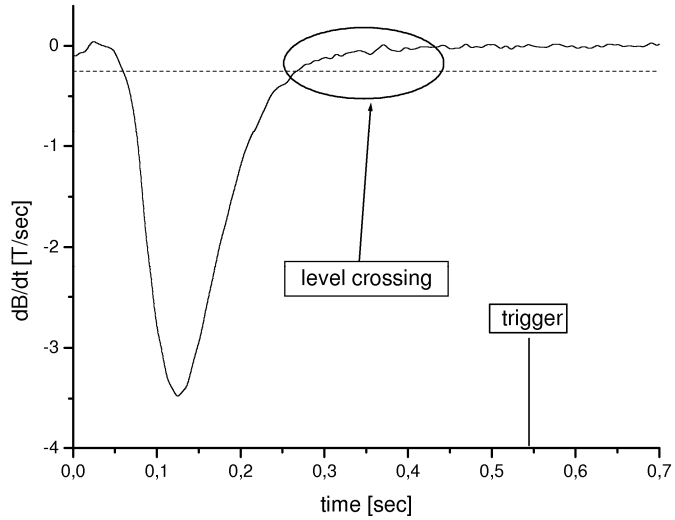

Figure 9: A typical rate of polarization field vs time at the level crossings (obtained with numerical derivation of the measured B(t) dependence). The dashed line is the recommended limit value.

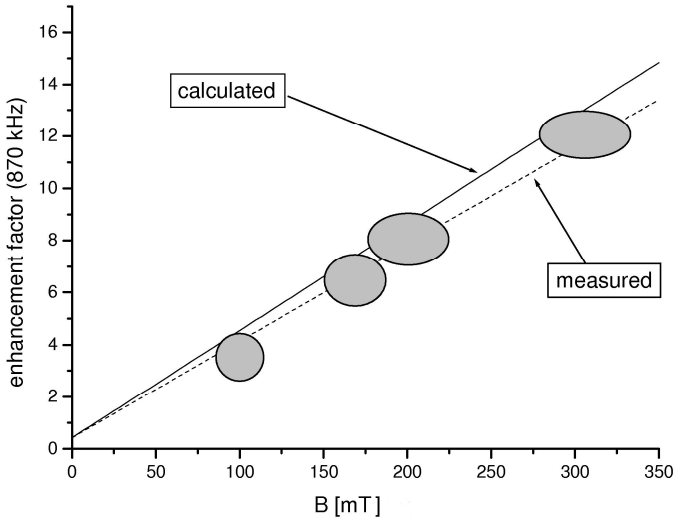

Figure 10: The signal intensity enhancement factor for the ν^+ (870 kHz) line in TNT at room temperature. The measured uncertainties, denoted by the ellipsoidal surfaces, are mainly due

to the dimensions of the sample and very inhomogeneous polarization magnetic field obtained with the NdFeB permanent magnet.

With polarization enhanced NQR and the proper selection of measuring pulse sequences, the s/n ratio of NQR signals can be increased up to three orders of magnitude. The required measuring time was thus adequately reduced [27, 28]. The multi-pulse pulse spin-locking (PSL) sequence applied in our experiments was: $\alpha_0 - (\tau - \alpha_{90} - \tau -)_n$, where n refers to the number of pulse-train repetitions and the pulse width α was chosen to optimize the signal. The sequence allowed several echoes in a single shot and thus effectively enhanced the s/n ratio with averaging them within the single shot. A typical time response of the detector is given on Fig. 11. For the resolution in the frequency space around 500 Hz usually 10 to 20 echoes could be averaged in one shot. The single shot ^{14}N signals at 842, 844 and 848 kHz in the central part of the NQR spectrum of 15 g of TNT at room temperature are shown in Fig. 12. The total measuring time for proton polarization, demagnetization and PSL sequence was about 15 s. 15 echoes in the single pulse sequence (single shot) were averaged. A sharp low pass filter of 5 kHz, 12 dB/octave at the receiver output was used. The polarization field was ~ 250 mT.

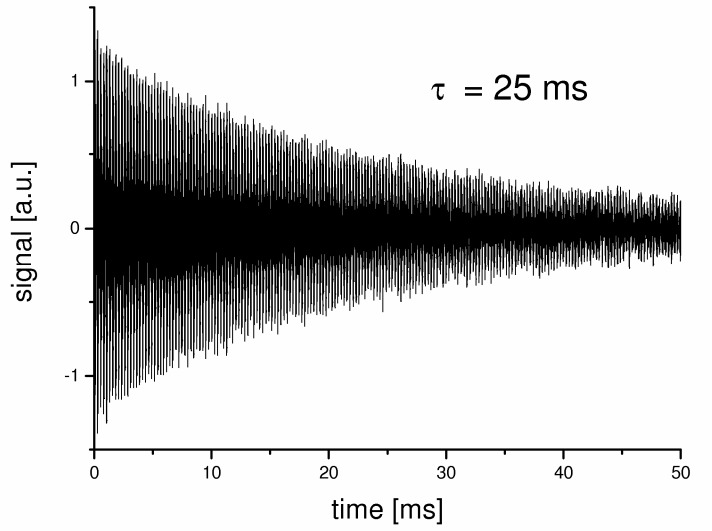

Figure 11: A train of 200 echoes showing the typical decay time approx. 25 ms (~300 averages).

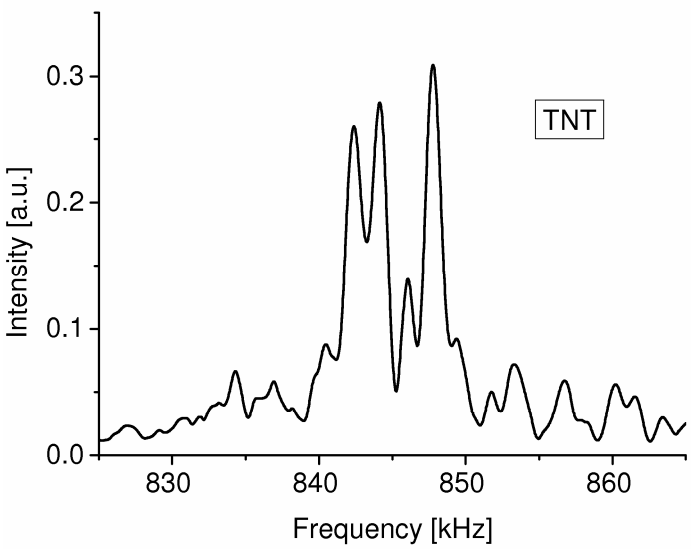

Figure 12: The central part of the ^{14}N NQR spectrum (signals at 842, 844 and 848 kHz) in pure monoclinicTNT with reference frequency 845 kHz filtered, with a sharp LP filter at the receiver output, obtained from a single shot experiment.

In relatively short time the complete ^{14}N NQR TNT spectrum of sufficient quality can be obtained (Fig 13). With the reduced resolution we can apply pulse sequences with much shorter pulse distances and increase the number of echoes for averaging (depending on the echo effective decay time). Namely, for the detection of an illicit substance the sensitivity is more important than the resolution. Fig 14 shows two examples of single shot ^{14}N NQR signals in monoclinic TNT where pulse separations are 2000 μs and 400 μs. 50 and 400 echoes were averaged respectively.

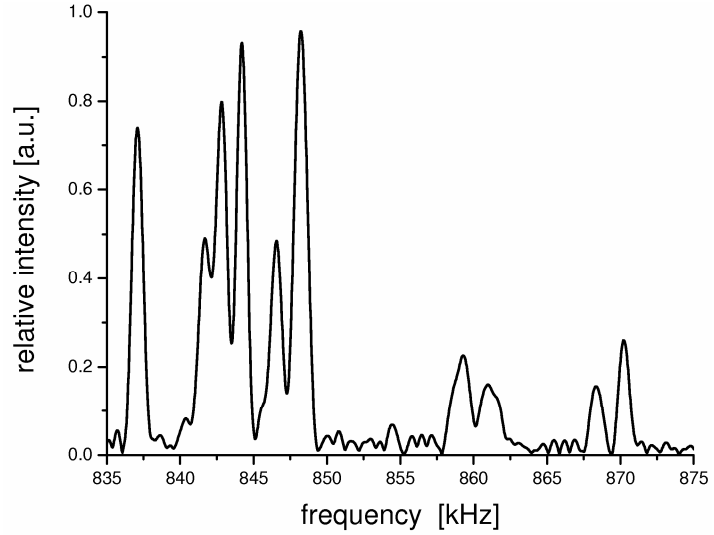

Figure 13: ν^+ part of ^{14}N NQR spectrum in an old sample of TNT where the mixture of two phases monoclinic/orthorhombic (approx. 50%/50%) can clearly be resolved. With polarization enhancement such a spectrum can be obtained in 10 to 15 minutes (~30 averages).

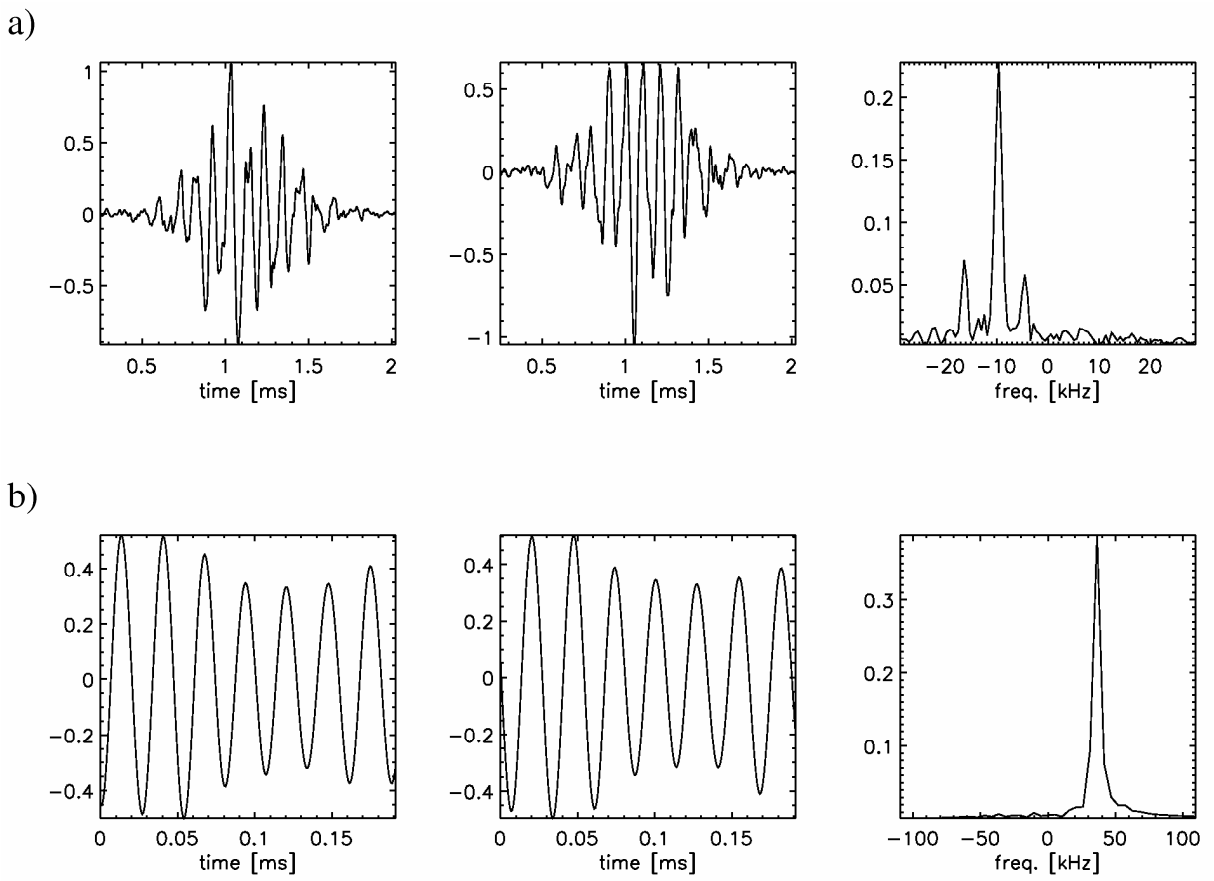

Figure 14: Two examples of single shot ^{14}N NQR signals in TNT obtained from averaged echoes: a) the pulse separation time 2τ = 2000 μs, average of 50 echoes and b) the pulse separation time 2τ = 400 μs, average of 400 echoes Only the second half of echoes is averaged in b), because of the after pulse detection dead time.). In a) we can resolve 837 and 848 kHz lines while the 842 and 844 lines appear as a broader single line in the middle. In b) the resolution in frequency space is so low that only one line can be observed, but with much higher signal/noise ratio. The receiver reference frequencies were: 855 kHz a) and 820 kHz b). The three panels from left to right: absorption, dispersion and power spectra.

We can conclude with: Our results demonstrate that polarization enhanced single shot pulse spin-locking detection of ^{14}N NQR is fast and sensitive enough to be applied for routine detection of explosives in, e. g., mail services, customs control and in prevention of terrorist actions, as well as in the pharmaceutical industry for nondestructive chemical analysis of solid samples and for polymorph determination.

Acknowledgement:

This research was supported by: 1) the Slovenian Research Agency of the Ministry of Higher Education, Science and Technology (Grant No. 3311-04-828010) and 2) NATO Science for Peace (Grant No. SfP-978007).

References

[1] Grechishkin V.S. and Sinjavsky N.J.: Phys. Usp. **40**, 393 (1997)
[2] Yesinowski J.P., Buess M.L., Garroway A.N.: Anal. Chem. **67**, 2256 (1995)
[3] Grechishkin V.S.: Appl. Phys. A: Solids Surf. **55**, 505 (1992)
[4] Garroway A.N., Buess M.L., Miller J.B., Suits B.H., Hibbs A.D., Barrall G.A., Matthews R., Burnett L.J.: IEEE Trans. Geosci. Remote Sens. **39,** 1108 (2001)
[5] Smith J.A.S., Deas R.M., Gaskell M.J.: *International Conference on Requirements and Technologies for the Detection, Removal and Neutralization of Landmines and UXO,* 15-18 September 2003 (Vrije Universiteit Brussels, Belgium, Vol. 2, p. 715 (2003)
[6] Smith J.A.S.: Chem. Soc. Rev. **15**, 225 (1986)
[7] E. Balchin E., Malcolme-Lawes D.J., Poplett I.J.F., Rowe M.D., Smith J.A.S., Pearce D.E.S, Wren S.A.C.: Anal. Chem. **77**, 3925 (2005)
[8] Blinc R., Seliger J., Zidansek A., Zagar V., Milia F., Robert H.: Solid State Nucl. Magn. Reson. **30**, 61 (2006)
[9] Seliger J., Blinc R., Mali M., Osredkar R., Prelesnik A.: Phys. Rev. B **11**, 27 (1975)
[10] Slusher R.E. and Hahn E.L.: Phys. Rev. **166,** 332 (1968)
[11] Blinc R., Seliger J., Arcon D., Cevc P., Zagar V.: Phys. Stat. Sol. A **180**, 541 (2000)
[12] Nolte M., Privalov A., Altmann J., Anferov V., Fujara F.: J. Phys. D **35,** 939 (2002)
[13] Seliger J., V. Zagar V., R. Blinc R.: J. Magn. Reson., Ser. A **106**, 214 (1994)
[14] Kruk D., Altmann J., Fujara F., Gaedke A., Nolte M., Privalov A.F.: J. Phys.: Condens. Matter **17**, 519 (2005)
[15] Thurber K.R., Sauer K.L., Buess M.L., Klug C.A., J.B. Miller J.B.: J. Magn. Reson. **177,** 118 (2005)
[16] Luznik J. Pirnat J. and Trontelj Z.: Solid State Commun. **121,** 653 (2002)
[17] Blinc R., Apih T., Seliger J.: Appl. Magn. Reson. **25**, 523 (2004)
[18] Grechishkin V.S., Anferov V.P., Sinjavsky N.J.: Adv. Nucl. Quadrupole Reson. **5**, 13 (1983)
[19] Mikhaltsevitch T. and Beliakov A.V.: Solid State Commun. **138**, 409 (2006)
[20] Abragam A.: The Principles of Nuclear Magnetism, Clarendon Press, Oxford, 1961
[21] Goldman M.:Spin Temperature and Nuclear Magnetic Resonance in Solids, Oxford University Press, 1970
[22] Edmonds D.T.: Phys. Rep. **29,** 233(1977)
[23] Das T.P., Hahn E.L.: Nuclear Quadrupole Resonance Spectroscopy, Academic Press Inc., New York - London,1958
[24] Marino R.A., Connors R.F.: J. Mol. Struct. **111**, 323(1983)
[25] Deas R.M., Gaskell M.J., Long K., Pierson N.F., Rowe M.D., Smith J.A.S.: Proc. SPIE **5415,** 510 (2004)
[26] Naito A., Root A., McDowell C.A.: J. Phys. Chem. **95,** 3578 (1991)
[27] Luznik J., Pirnat J., Jazbinsek V., Apih T., Gregorovic A., Blinc R., Seliger J., Trontelj Z.: Appl. Phys. Lett. **89**, 123509 (2006)
[28] Luznik J., J. Pirnat J., Jazbinsek V., Apih T., Gregorovic A., Blinc R., Seliger J., Trontelj Z.: J. Appl. Phys. **102**, 084903 (2007)

Table

No.	ν^+[kHz]	ν^- [kHz]	ν^0 [kHz]	η
1	870	714	156	0.295
2	859	751	108	0.201
3	848	739	109	0.206
4	844	714	130	0.250
5	842	769	73	0.136
6	837	743	94	0.178

Table1: ^{14}N NQR frequencies and asymmetry parameters for monoclinic TNT at room temperature

Figure captions

Figure 1: The quadrupole energy levels and allowed transitions for a spin 1 nucleus

Figure 2: The occupation number alteration of different energy levels in a three step cross-polarization transfer. α, β and γ denote the increments of the population differences after each level crossing.

Figure 3: Proton-nitrogen level crossing polarization enhancement and pulsed spin-locking detection procedure (schematic).

Figure 4: ν^+ part of ^{14}N NQR spectrum of predominantly monoclinic TNT. Six lines for monoclinic TNT can be resolved: 837 kHz, 842 kHz, 844 kHz, 848 kHz, 859 kHz and 870 kHz. This spectrum was obtained from nine averages in three sets where only the transmitter frequency was changed in three steps (837 kHz, 846 kHz and 865 kHz). The reference frequency Rx was constant at 855 kHz. A polarizing field of about 250±50 mT was used for this polarization enhancement experiment.

Figure 5: Calculated enhancement factor vs the polarizing field for ν^+, ν^- and ν^0 lines in TNT. Average enhancement factors for ν^+, ν^- and ν^0 are given assuming that ν^+ and ν^- transitions are grouped around 850 kHz and 750 kHz, respectively.

Figure 6: Average signal intensity vs polarization time for the triplet (842, 844 and 848 kHz) NQR line in the polarizing field 400±50 mT. The characteristic time for an exponential fit to the measured data is 16 s. This time is approximately equal to the proton spin-lattice relaxation time T_1.

Figure 7: A typical time dependence of the magnetic field at the place of the sample.

Figure 8: Average ^{14}N NQR signal intensity vs trigger delay time for the triplet line (842, 844 and 848 kHz) in TNT at room temperature.

Figure 9: A typical rate of polarization field vs time at the level crossings (obtained with numerical derivation of the measured B(t) dependence). The dashed line is the recommended limit value.

Figure 10: The signal intensity enhancement factor for the ν^+ (870 kHz) line in TNT at room temperature. The measured uncertainties, denoted by the ellipsoidal surfaces, are mainly due to the dimensions of the sample and very inhomogeneous polarization magnetic field obtained with the NdFeB permanent magnet.

Figure 11: A train of 200 echoes showing the typical decay time approx. 25 ms (~300 averages).

Figure 12: The central part of the ^{14}N NQR spectrum (signals at 842, 844 and 848 kHz) in pure monoclinic TNT with reference frequency 845 kHz filtered, with a sharp LP filter at the receiver output, obtained from a single shot experiment.

Figure 13: ν^+ part of ^{14}N NQR spectrum in an old sample of TNT where the mixture of two phases monoclinic/orthorhombic (approx. 50%/50%) can clearly be resolved. With polarization enhancement such a spectrum can be obtained in 10 to 15 minutes (~30 averages).

Figure 14: Two examples of single shot ^{14}N NQR signals in TNT obtained from averaged echoes: a) the pulse separation time 2τ = 2000 μs, average of 50 echoes and b) the pulse separation time 2τ = 400 μs, average of 300 echoes Only the second half of echoes is averaged in b), because of the after pulse detection dead time.). In a) we can resolve 837 and 848 kHz lines while the 842 and 844 lines appear as a broader single line in the middle. In b) the resolution in frequency space is so low that only one line can be observed, but with much higher signal/noise ratio. The receiver reference frequencies were: 855 kHz a) and 820 kHz b). The three panels from left to right: absorption, dispersion and power spectra.